

DESIGN, ASSEMBLY AND COMMISSIONING OF A TEST APPARATUS FOR CHARACTERIZING THERMAL INTERFACE MATERIALS

J.R. Culham*, P. Teertstra † I. Savija‡ and M.M. Yovanovich§

Microelectronics Heat Transfer Laboratory
Department of Mechanical Engineering
University of Waterloo
Waterloo, Ontario, Canada N2L 3G1
<http://www.mhtlab.uwaterloo.ca>

ABSTRACT

While thermal interface materials (TIMs), such as greases, compliant polymers, metallic foils and phase change materials, are commonly used in most electronic and microelectronic applications their in-situ thermomechanical characteristics are not well understood. Analytical models are available for idealized surface geometries, including conforming rough surfaces and non-conforming, smooth surfaces, but models are typically not available for real surfaces that combine both surface roughness and waviness, especially for interfaces that incorporate interstitial materials to promote compliance. As a result, thermal interface materials are usually characterized experimentally, in adherence to guidelines described in ASTM standard D 5470-95 which does not provide for changes in material thickness during the application of a load.

This paper details the design and construction of a test apparatus that exceeds all specifications stipulated in ASTM D 5470-95 and can be used to accurately characterize thermal interface materials, including the precise measurement of changes in in-situ materials thickness resulting from loading and thermal expansion.

KEY WORDS: thermal interface materials (TIMs), test apparatus, contact resistance, in-situ thickness measurement, phase change materials, metallic foils, polymeric materials

NOMENCLATURE

A	=	cross sectional area, m^2
F	=	applied load, N
k	=	thermal conductivity, W/mK
P	=	interface pressure, MPa
Q	=	heat flow rate, W
R	=	thermal resistance, K/W
RTD	=	resistance temperature detector
t	=	thickness, m
\bar{T}_m	=	mean joint temperature, K
ΔT	=	temperature difference, K
TIM	=	thermal interface material
Δx	=	axial distance between RTDs, m

Subscripts

AR	=	as received
Al_{2024}	=	aluminum 2024 bar stock
$bulk$	=	bulk
c	=	contact
g	=	gap
$i, i1, i2$	=	interface
j	=	joint
$last$	=	RTD adjacent to interface

INTRODUCTION

The heat transfer path established between heat producing electronic components and the surrounding cooling medium typically consists of a complex network of various materials and interfaces that resist the transport of thermal energy and lead to increased temperature levels throughout the thermal circuit. As power dissipation levels

*Associate Professor, Director MHTL

†Research Engineer

‡M.A.Sc. Candidate

§Distinguished Professor Emeritus

are increased, the overall resistance in this network must be reduced to maintain heat sensitive components, such as IC junctions, at or below safe operating temperatures. Most electronic systems now employ some form of TIM to minimize interface resistance by replacing the air contained in the gaps at non-conforming interfacial boundaries with higher conductivity materials such as greases, compliant polymers, metallic foils or phase change materials.

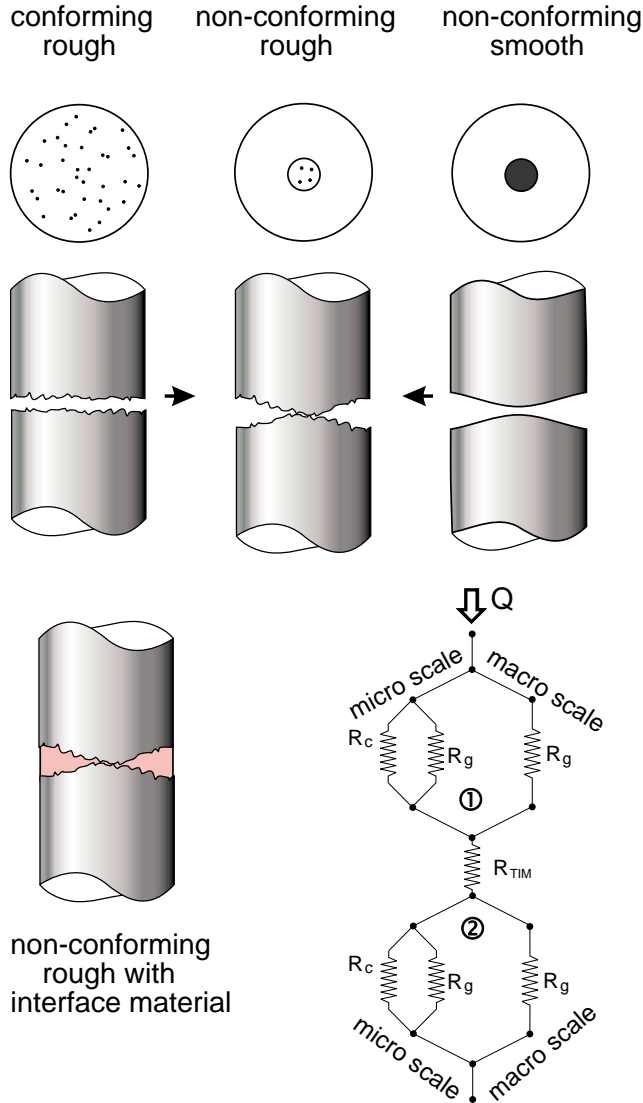


Fig. 1: Contacting Surface Geometries

The thermal interface formed between two real surfaces consists of many discrete microcontact spots resulting from contacting surface asperities with the majority of the apparent contact interface consisting of interstitial gaps formed between the asperities or due to surface waviness, as shown in Fig. 1. The overall interface resistance for a non-conforming, rough surface incorporating a TIM can be characterized using a seven resistor circuit as shown in Fig. 1. The resistors are used to represent the contact

and gap resistances for the two interfaces on either side of the interface material as well as the bulk resistance of the interface material. A simpler circuit, using as few as two resistors is possible for materials such as grease, where the grease fully wets the two surfaces and the load is fully supported by the contact asperities.

In order to quantify the joint resistance it is necessary to use models for the individual resistor elements that combine the mechanical, geometric and thermal behavior of the joint as a function of material surface characteristics, microhardness, applied load and material properties. While numerous authors have presented physical models for conforming rough surfaces [1,2] and non-conforming smooth surfaces [3,4] no comprehensive models currently exist for non-conforming rough surfaces with interface materials, which are representative of the geometry found in real contact interfaces. Savija et al. [5] presented an extensive review paper of thermal conductance models, including those dealing with enhancement materials. They concluded that the vast majority of the papers in this field are based on empirical studies that provide only limited use as a general modeling procedure. This conclusion underscores the need for a more controlled experimental test procedures that provide the basis for general, analytical models to predict the joint conductance in real contacts with thermal interface materials.

This paper will detail the design and construction of a test apparatus for characterizing TIMs under a wide range of applied loading and temperature conditions. The apparatus is designed to meet all requirements stipulated in ASTM standard D 5470-95 [6] and to exceed these requirements by varying loading conditions, limiting extraneous heat losses and varying mean interface temperatures over the range typically found in electronic applications. ASTM D 5470-95 is the standard procedure used to determine the thermal conductivity or interface resistance associated with “thin thermally conductive solid electrical insulation materials”. The standard is designed to:

- measure the thermal impedance (resistance) of thin electrical insulation materials in a thickness range of 0.02 to 10 mm
- calculate the “apparent thermal conductivity” based on the thickness as manufactured, *not* the in-situ thickness resulting from changes due to loading or thermal expansion
- calculate one thermal conductivity at $\bar{T}_m = 50\text{ }^\circ\text{C}$ and $P = 3.0 \pm 0.1\text{ MPa}$

subject to:

- non-conformities in contacting surfaces due to either roughness or waviness being less than $0.4\text{ }\mu\text{m}$

- steady state conditions, defined as having successive temperature readings over a 15 min interval within 0.2 °C

INTERFACE MATERIALS

Savija et al. [5] presented a comprehensive review of various models for determining the thermal conductance of joints with and without enhancement materials. Their paper details modeling procedures for fluidic materials such as greases, oils, phase change substances and other materials that perfectly wet the contacting interfaces as well as non-fluidic materials such as polymers, adhesives and metallic coating and foils that may not be in perfect contact with the substrate surfaces. It is clear from this review article that the wide range of mechanical properties associated with interface materials necessitates special consideration when testing for thermal conductance.

The various materials discussed in the Savija et al. review article can be classified into four categories based on the expected deflection of the TIM under an applied compressive load.

1. **Type 1:** Materials requiring a minimal clamping force, such as greases, phase change materials, adhesives, liquids, and putties.
2. **Type 2:** Materials that will deform (displace) 10% under a clamping force (Durometer scale 00)
3. **Type 3:** Materials that are deformed less than 10% under a clamping force; hard rubber (Durometer scale A)
4. **Type 4:** Thermally conductive materials such as plastics and ceramics that require high clamping forces (Durometer scale D)

TEST PROCEDURE

Joint Resistance

The ASTM standard D 5470-95 calls for an indirect measurement of the “as received” thermal conductivity, denoted as k_{AR} , through the physical measurement of the total thermal resistance of a mechanical joint.

$$k_{AR} = \frac{1}{R_j \cdot t_{AR}} \quad (1)$$

The resistance to heat flow across the TIM, R_j , is measured by determining the temperature drop across the joint for a known heat flow rate. The ASTM standard recommends the use of a guarded heater and a reference calorimeter to monitor the steady heat flow through a test column,

where the temperature drop across the sample is determined by extrapolating point temperatures measured on either side of the test sample. Although not stipulated in the standard, a modified version of the guarded heater setup can be obtained by using a test column, as shown in Fig. 2, contained within a vacuum chamber to minimize heat losses attributed to conduction or convection.

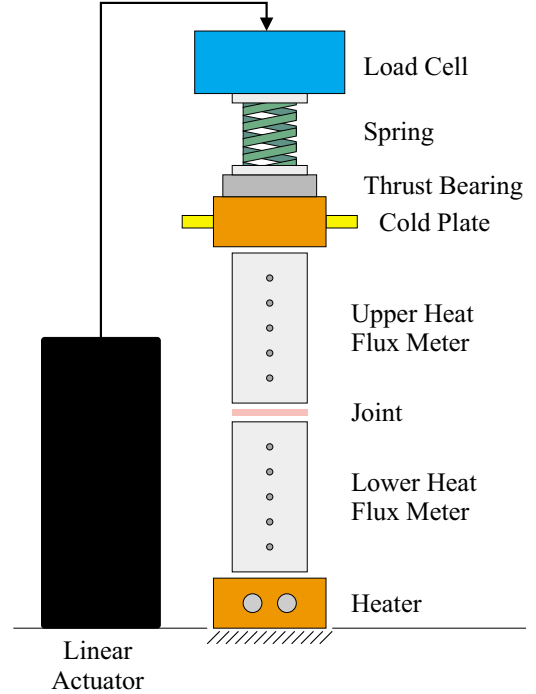


Fig. 2: Apparatus for Measuring the Resistance of Thermal Interface Materials

The ASTM test standard mandates that the thermal resistance of the test sample should be measured with an applied interface pressure of 3 MPa to minimize the interface resistances formed between the test sample and the calorimeter or heat flux meters. As shown in the thermal circuit in Fig. 1, the heat flow in the test column must pass through a parallel path consisting of gap and contact resistances associated with both macro-scale waviness or out-of-flatness and micro-scale roughness. Equations 2-4 provide a simple procedure for calculating the overall joint resistance as a series summation of the two interface resistances and the bulk resistance of the TIM.

$$R_j = R_{i1} + R_{TIM} + R_{i2} \quad (2)$$

where

$$R_{TIM} = \left(\frac{t}{kA} \right)_{TIM} \quad (3)$$

$$\frac{1}{R_i} = \left(\frac{1}{R_c} + \frac{1}{R_g} \right)_{micro} + \left(\frac{1}{R_c} + \frac{1}{R_g} \right)_{macro} \quad (4)$$

The interface resistance, R_i is based on the parallel path resistance consisting of the gap and contact resistance associated with micro-scale roughness and macro-scale waviness.

Depending on the quality of the interface formed between the heat flux meters and the TIM, the joint resistance can be significant and when incorporated into the calculation of the joint resistance and subsequently the calculation of the thermal conductivity, will lead to an overestimation of the thermal resistance and an underestimation of the thermal conductivity. In light of this, ASTM standard D 5470-95 calls for an interface pressure of 3 MPa and a surface roughness of less than 0.4 μm . By minimizing the joint resistance the predominant resistance at the interface is the bulk resistance of the TIM. Unfortunately, as high loads are applied to compliant materials, the thickness changes and the use of an “as-received” thickness no longer provides an accurate measure of thermal conductivity.

If we assume that the load characteristics and the surface finish of the joint are sufficient to minimize the effect of interface resistance, then the joint resistance can be written as

$$R_j = R_{TIM} = \left(\frac{t}{kA} \right)_{TIM} = \frac{\Delta T_j}{Q} \quad (5)$$

and the thermal conductivity of the interface material can be determined as

$$k_{TIM} = \frac{Q}{\Delta T_{TIM}} \cdot \frac{t_{TIM}}{A_{TIM}} \quad (6)$$

where the thickness of the interface material, t_{TIM} is the in-situ thickness of the TIM including any changes resulting from loading and thermal expansion.

Heat Flow Rate

The introduction of a heat flow rate into the test column is easily accomplished using cartridge heaters as shown in Fig. 2. However, maintaining a steady heat flow rate, independent of surrounding conditions is not always achievable given the likelihood of fluctuations in heat losses associated with changes in the surrounding conditions during the duration of a test. Two approaches are traditionally used to stabilize or eliminate heat losses, i) a guarded heater where surrounding conditions are controlled through a secondary heater and ii) a vacuum environment where conduction and convection heat losses are minimized and radiation heat losses can be controlled through a radiation shield. The latter approach has been adopted for this test apparatus. A vacuum pressure of 1×10^{-4} torr is sufficient to minimize any extraneous heat losses from the test column.

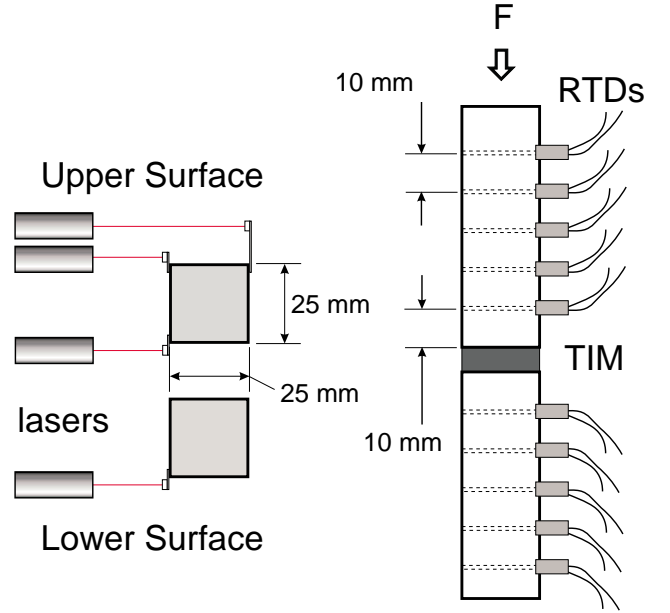


Fig. 3: Heat Flux Meters and Laser/Detector Configuration

The heat flow in the test column can be measured using a heat flux meter, as shown in Fig. 3, where five RTDs are spaced on 10 mm centers in each flux meter. If we assume that the heat flow is uniform across the cross section of the 25 mm \times 25 mm Al 2024 bar stock, then by measuring the temperature gradient in the axial direction and knowing the thermal conductivity of the Al 2024 an accurate measure of heat flow rate can be calculated as

$$Q = -k_{Al2024} A \frac{dT}{dx} \quad (7)$$

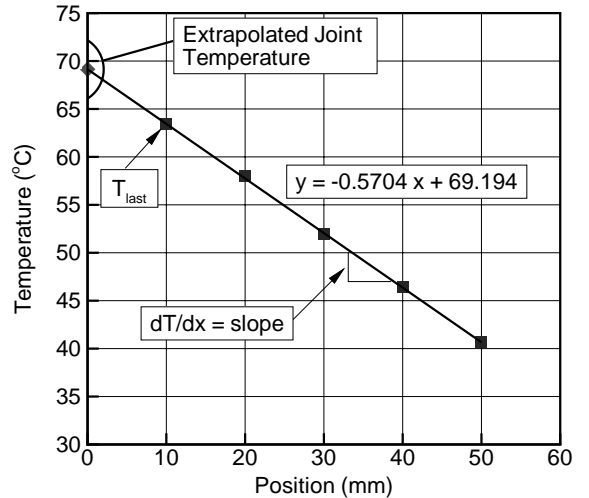


Fig. 4: Heat Flux Meter Temperature Gradient for Estimating Heat Flow Rate

As shown in Fig. 4, by plotting temperatures at known locations, the temperature gradient in the heat flux meter

Table 1: Temperature Measurement Options [7]

	Thermocouple	Platinum RTD	Semiconductor	Thermistor
Sensor	thermo electric dissimilar metals	platinum wire or flat film resistor	semiconductor junction	ceramic (metal oxide)
Accuracy	0.5 °C	0.1 °C	0.5 °C	0.05 °C
Stability	prone to aging	0.05 °C/yr	1.0 °C/yr	0.02-0.2 °C/yr
Linearity	non-linear	linear	linear	exponential
Response Time	0.1 - 10 s	1 - 50 s	5 - 50 s	0.5 - 10 s
Cost	low	high	moderate	moderate

can be accurately determined using a simple least squares regression routine. By performing a similar procedure below and above the test sample, an estimate of the energy balance across the interface can be determined. If the balance is reasonable, then a simple arithmetic average of the two measured values of heat flow rate can be used as the heat flow rate in the test column. Typical energy balances between the upper and lower heat flux meters of $\pm 3\%$ are considered acceptable.

Interface Temperatures

The heat flux meters serve a second important function in addition to determining the heat flow rate in the column and that is to determine the temperature change across the TIM. As shown in Fig. 4, the measured axial temperature profile in the flux meters can be used to linearly extrapolate to the surface of the flux meter in contact with the test sample. If the interface resistance is negligible, the temperature difference between the flux meter and the sample is negligible and the extrapolated flux meter temperature can be used as the surface temperature of the sample as follows:

$$T_{TIM} = T_{last} \pm \frac{dT}{dx} \cdot \Delta x \quad (8)$$

Through this extrapolation procedure with the lower and upper flux meters the temperature change across the sample, ΔT_{TIM} can be determined as

$$\Delta T_{TIM} = T_{TIM,lower} - T_{TIM,upper} \quad (9)$$

While ASTM D 5470-95 does not specifically stipulate the level of accuracy required for temperature measurement, it does make repeated reference to maintaining temperatures to within $\pm 0.2 K$ in the test column. In order to achieve this level of control, temperature measurement capabilities must be better than $\pm 0.2 K$. As shown in Table 1, sensor characteristics for the four common temperature sensing devices offer a mixed range of specifications.

Given the accuracy, stability and linearity of the RTDs, they were chosen as the preferred method of measuring temperature in the test column. While the cost is relatively high, the long term stability of the RTDs makes them the

clear winner for accurate, repeatable temperature measurement.

In-situ Thickness

As shown in Eq. 3, the measured joint resistance and the thickness of the TIM are directly related through the thermal conductivity of the interface material and the cross sectional area of the test sample. The ASTM test standard recommends that the thermal resistance, R_{TIM} should be measured in-situ, subject to an applied load of 3 MPa and a mean interface temperature of 50 °C while the thickness is an as received measurement at room temperature and independent of a load. However, given the compliant nature of most TIMs, as reflected in their relatively low value of Young's modulus, it is safe to assume that compressive loading will result in a reduction in the mean thickness of the sample. Similarly, increasing the sample temperature from room temperature to 50 °C will result in a change in the thickness associated with thermal expansion. While these two effects may cancel out somewhat, it is highly unlikely that the in-situ thickness will correspond to the as received thickness and as a result the estimation of the material conductivity will be inaccurate.

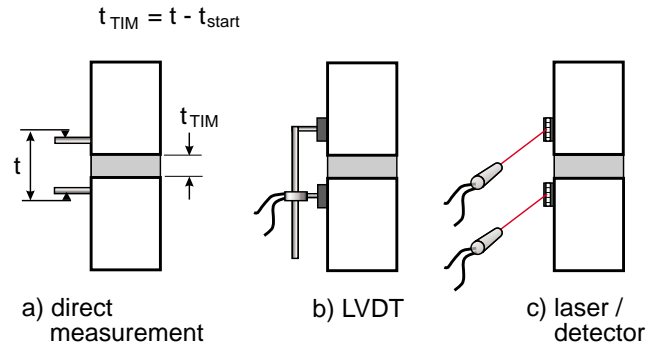


Fig. 5: In-situ Thickness Measurement Options

In order to accurately determine the thermal conductivity of TIMs it is important to measure the sample thickness and the thermal resistance under identical loading and thermal conditions. A number of options were considered for measuring the in-situ thickness, including:

1. direct measurement using a vernier or a micrometer

2. LVDT - Linear Variable Differential Transformer
3. laser-based system with a target mounted on the sample

Direct measurement: As shown in Fig. 5a, the in-situ thickness of the interface material is determined by measuring the offset between the lower and upper heat flux meters, t , using two surface mounted, measuring guide pins. Prior to inserting the interface material, the upper and lower flux meters are placed in direct contact with each other and the initial offset between the guide surfaces, t_{start} , is determined using a vernier or a micrometer. Once the interface material surface is inserted, the process is repeated when the sample reaches a thermal steady state, with the in-situ thickness, t_{TIM} , being the difference between the steady state reading and the initial offset measurement.

While the procedure is inexpensive, easy to perform and repeatable there are several limitations that preclude its use for this type of experimental test fixture. First, in order to have easy access to the guide surfaces, the thermal test must be conducted at atmospheric conditions. Since it was decided to use a vacuum environment surrounding the test fixture to minimize heat losses to the surrounds (a guarded heater system was considered and rejected), access to the guide surfaces will not be available during the thermal testing procedure. In addition, a measurement resolution of $100 \mu m$ for the best micrometer available was well outside the required accuracy of $1 \mu m$ necessary for small changes in thickness associated with thin film materials. And finally, because the measurement procedure requires some direct contact with the measurement guide surfaces, there is a possibility of altering the thermal steady state and the measurement of the thermal resistance. For the reasons cited here this procedure was rejected.

LVDT: The linear variable differential transformer is a non-intrusive measurement procedure that relates the electrical output from an electromechanical transducer to linear displacement. As shown in the schematic in Fig. 5b, a voltage signal is produced as a non-magnetic core attached to the upper surface is moved through the core of the LVDT attached to the lower sample. There is no direct contact between the upper and lower surfaces and no thermal bridging. The output voltage from the transducer, which is directly related to linear displacement of the samples, can be easily monitored within the vacuum environment of test apparatus. The cost of measuring a single point, including the LVDT, core and the signal amplifier, is approximately \$US1500.

Given the small dimensions of the LVDT and the core, it is very difficult to mount the necessary hardware on the upper and lower surfaces without disrupting the physical integrity of the experiment. In order to measure changes in sample thickness in the range of $1 \mu m$, the nominal linear range of the LVDT must be constrained to approximately

$0.25 - 0.64 \text{ mm}$. This implies that the core must be placed within this starting range in order to accurately measure $1 \mu m$ changes in thickness. It was felt that given the difficulties with mounting the required hardware and the physical limitations associated with setting the initial placement of the core and the LVDT, that this arrangement was not practical.

Laser: As shown in the schematic in Fig. 5c and the photograph in Fig. 6, the laser/detector system proposed for measurement of in-situ material thickness consists of three basic components for each sampling point, i) a 5 mW laser with a wavelength of 670 nm collimated to a beam width of $100 \mu m$ at an offset distance of 100 mm , ii) a $6 \text{ mm} \times 1 \text{ mm}$ one-dimensional PSD (position sensitive detector) with a total weight of approximately 1 gram , and iii) a signal processing card that produces a voltage in the range of $\pm 10 \text{ V}$ for the full range of the detector. The quoted position resolution for the laser/detector system is $0.2 \mu m$.

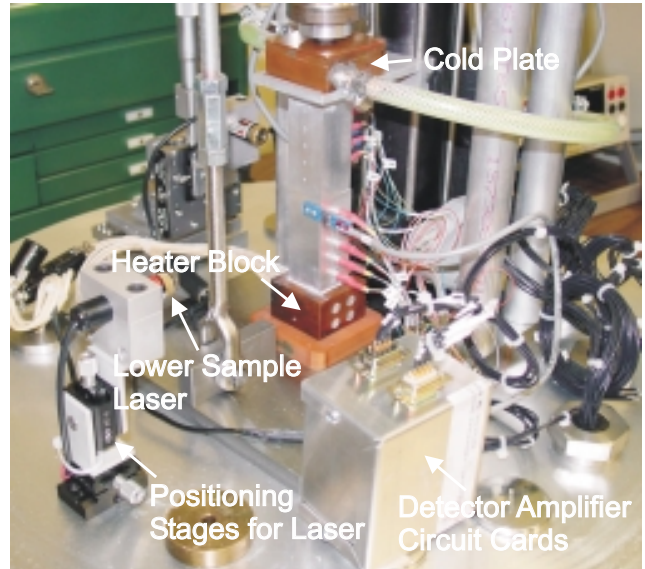


Fig. 6: Laser/detector Measurement System

FINAL ASSEMBLY

The components described above have been configured into a final test assembly as shown in Figs. 7 and 8.

Figure 7 shows a close up view of the test configuration for a compliant material where the in-situ thickness is measured by monitoring the differential thickness between the upper and lower laser/detector systems. The test configuration shown in Fig. 8 is for a thermal grease where a precise thickness is maintained with a small piece of shim stock at each corner of the joint. As a result, the in-situ thickness is maintained throughout the duration of the test and the laser/detector measurement system is not needed in this instance.

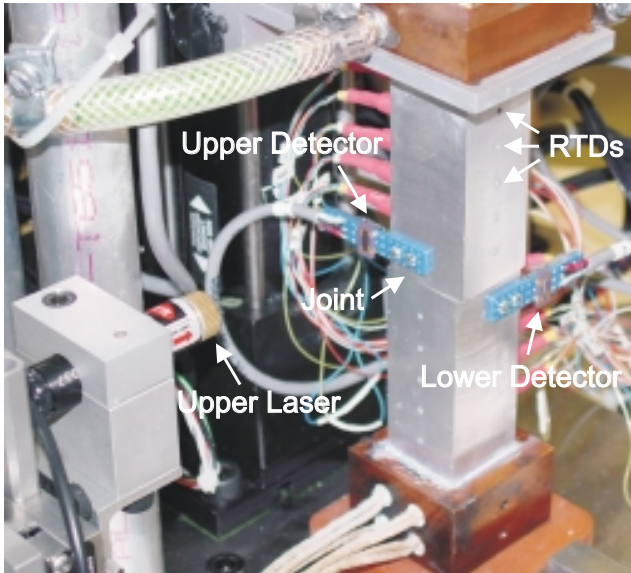


Fig. 7: Testing of a Compliant Material

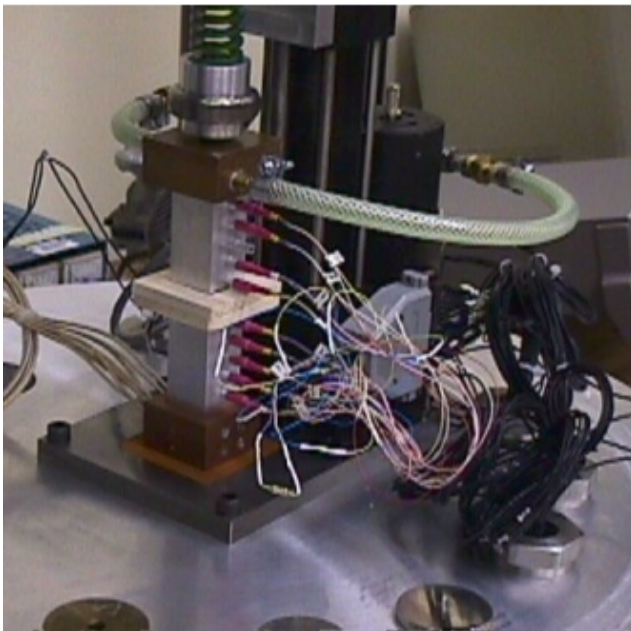


Fig. 8: Testing of a Thermal Grease

The initial test configuration for measurement of in-situ thickness consists of two laser/detectors as shown in Fig. 5c. In this situation the contacting surfaces of the flux meters are assumed to remain parallel throughout the test and the lasers monitor a uniform change in thickness across the joint. In the event that the surfaces of the heat flux meters do not remain parallel throughout the test process a four point laser detector system as shown in Fig. 3 can be used to measure the non-parallel movement of the upper sample as the load is applied. In both situations the lower sample which is attached directly to the base-plate of the vacuum chamber is assumed to be rigid.

Once assembled the data acquisition and control of the test apparatus is performed using a Kiethley 2700 data logger with 40 analog inputs, 20 analog outputs and two digital I/O channels. The testing sequence is fully automated using a Personal computer with a LabView interface to monitor all aspects of the testing, including convergence checking, test sequencing, limit controls and data collection.

The completed final assembly, including the baseplate for the vacuum bell jar, the test column and the pivot arm for maintaining axial loading, is shown in Fig. 9. The total cost of the unit including manufacture, materials, equipment and software was approximately \$24,000, with a parts inventory and cost summary given in the Appendix.

ACKNOWLEDGMENTS

The authors wish to acknowledge the financial support of the Natural Sciences and Engineering Research Council of Canada, the Centre for Microelectronics Assembly and Packaging, Materials and Manufacturing Ontario and R-Theta Inc. Mississauga ON. The assistance of Mr. Dave McClafferty, IBM Poughkeepsie, in the design of the laser/detector system is greatly appreciated.

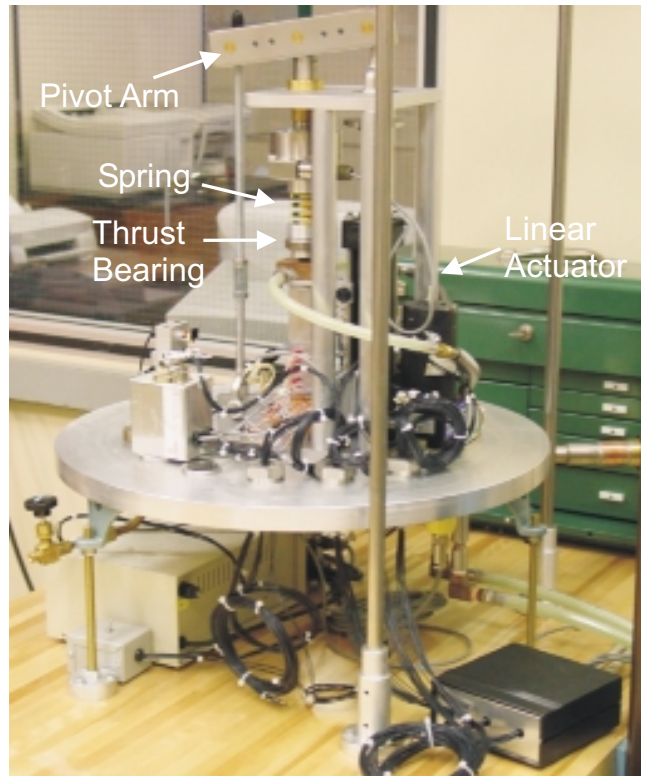


Fig. 9: Fully Assembled Test Apparatus

REFERENCES

1. Cooper, M., Mikic, B. and Yovanovich, M.M., "Thermal Contact Conductance," Journal of Heat and Mass Transfer, vol. 12, pp. 279-300, 1969.
2. Yovanovich, M.M., DeVaal, J.W. and Hegazy, A.A., "A statistical Model to Predict Thermal Gap Conductance Between Conformint Rough Surfaces," AIAA paper no. 82-0888, AIAA/ASME 3rd Joint Thermophysics, Fluids, Plasma and Heat Transfer Conference, St. Louis, Missouri, June 7-11, 1982.
3. Johnson, K.L., *Contact Mechanics*, Cambridge University Press, 1985.
4. Johnson, K.L., Greenwood, J.A. and Higginson, J.G., "The Contact of Elastic Wavy Surfaces," International Journal of Mechanical Sciences, 27, (401), 1985.
5. Savija, I., Culham, J.R., M.M. Yovanovich and Marotta, E.E., "Review of Thermal Conductance Models for Joints Incorporating Enhancement Materials," AIAA 2002-0494, 49th AIAA Aerospace Sciences Meeting and Exhibit, Reno, Nevada, January 14-17, 2002.
6. "Standard Test Method for Thermal Transmission Properties of Thin Thermally Conductive Solid Electrical Insulation Materials," ASTM D 5470-95, 1995.
7. Personnal communications with Jon Matheson, Hoskin Scientific Limited, Burlington, ON, Canada.

APPENDIX

Parts List	Cost \$US
Test Column	
1 - linear actuator, 800 lbs max.	\$1,585
10 - platinum RTDs	\$1,050
1 - 1000 lb. load cell	\$960
- cartridge heaters, current shunts, springs	\$110
Vacuum System	
1 - 18 inch by 18 inch pyrex bell jar w/ sealing gasket	\$1,500
1 - vacuum gauge controller w/ 1/8 inch gauge tube	\$780
1 - 1/2 HP, single phase, vacuum pump	\$1,875
3 - vacuum feed throughs	\$1,250
Data Acquisition & Control	
1 - 30V, 3 A DC power supply	\$250
1 - Kiethley 2700, w/ 7700 Analog Input Module w/ 7760 All-in-one Module	\$2,780
1 - Personal computer	\$800
In-situ Thickness Measurement	
4 - laser measurement system <ul style="list-style-type: none"> • 5mW red laser, wavelength 670 nm w/ universal voltage power supply • 1D position sensitive detector • signal processing circuit card 	\$3,075
1 - translation stage	\$720
Miscellaneous	
1 - 60 inch by 36 inch pedestal bench	\$400
1 - constant current source for RTDs	\$100
1 - constant temperature bath, 13 litres, 480 W, 7 litres per minute	\$2,400
- machining costs (base plate, flux meters, bell jar counter balance, etc.)	\$2,900
- material (base plate, etc)	\$1,000
- thrust bearing, cold plate,	\$250
Total	\$23,785